Monthly Notices
of the
ROYAL ASTRONOMICAL SOCIETY

MNRAS **487,** L81–L85 (2019)
Advance Access publication 2019 June 18

doi:10.1093/mnrasl/slz094

The absence of [C II] 158 μm emission in spectroscopically confirmed galaxies at $z > 8$

N. Laporte [1]★ H. Katz,[2] R. S. Ellis,[1] G. Lagache,[3] F. E. Bauer,[4,5,6] F. Boone,[7] A. K. Inoue [8,9] T. Hashimoto [9] H. Matsuo,[10] K. Mawatari[11] and Y. Tamura[12]

[1]*Department of Physics & Astronomy, University College London, London WC1E 6BT, UK*
[2]*Astrophysics, University of Oxford, Denys Wilkinson Building, Keble Road, Oxford OX1 3RH, UK*
[3]*Aix-Marseille Univ., CNRS, LAM, Laboratoire d'Astrophysique de Marseille, F-13388 Marseille, France*
[4]*Instituto de Astrofísica, Facultad de Física, Pontificia Universidad Católica de Chile Av. Vicuña Mackenna 4860, 782-0436 Macul, Santiago, Chile*
[5]*Millennium Institute of Astrophysics (MAS), Nuncio Monseñor Sótero Sanz 100, Providencia, Santiago, Chile*
[6]*Space Science Institute, 4750 Walnut Street, Suite 205, Boulder, CO 80301, USA*
[7]*Institut de Recherche en Astrophysique et Planétologie (IRAP), Université de Toulouse, CNRS, UPS, F-31400 Toulouse, France*
[8]*Department of Physics, School of Advanced Science and Engineering, Waseda University, 3-4-1, Okubo, Shinjuku, Tokyo 169-8555, Japan*
[9]*Waseda Research Institute for Science and Engineering, 3-4-1, Okubo, Shinjuku, Tokyo 169-8555, Japan*
[10]*National Astronomical Observatory of Japan, Mitaka, Tokyo 181-8588, Japan*
[11]*Institute for Cosmic Ray Research, University of Tokyo, 5-1-5, Kashiwa-no-ha, Kashiwa, Chiba 277-8582, Japan*
[12]*Division of Particle and Astrophysical Science, Graduate School of Science, Nagoya University, Nagoya 464-8602, Japan*

Accepted 2019 June 5. Received 2019 May 23; in original form 2019 April 25

ABSTRACT

The scatter in the relationship between the strength of [C II] 158 μm emission and the star formation rate at high redshift has been the source of much recent interest. Although the relationship is well established locally, several intensely star-forming galaxies have been found whose [C II] 158 μm emission is either weak, absent, or spatially offset from the young stars. Here we present new ALMA data for the two most distant gravitationally lensed and spectroscopically confirmed galaxies, A2744_YD4 at $z = 8.38$ and MACS1149_JD1 at $z = 9.11$, both of which reveal intense [O III] 88 μm emission. In both cases we provide stringent upper limits on the presence of [C II] 158 μm with respect to [O III] 88 μm. We review possible explanations for this apparent redshift-dependent [C II] deficit in the context of our recent hydrodynamical simulations. Our results highlight the importance of using several emission line diagnostics with ALMA to investigate the nature of the interstellar medium in early galaxies.

Key words: galaxies: evolution – galaxies: high-redshift – galaxies: starburst – early universe – submillimetre: galaxies.

1 INTRODUCTION

During the past few years the Atacama Large Millimetre/submillimeter Array (ALMA) has demonstrated its remarkable power by exploring the interstellar media (ISM) in galaxies in the reionization era. In addition to studies of extreme and rare dusty sub-millimetre galaxies at redshifts $z \simeq 5$–6 (e.g. Capak et al. 2015; Pavesi et al. 2018), the array has become the most reliable tool for spectroscopic confirmation of more typical distant star-forming galaxies (Inoue et al. 2016; Carniani et al. 2017; Laporte et al. 2017; Hashimoto et al. 2018, 2019; Smit et al. 2018; Tamura et al. 2019)

The two most prominent emission features targeted by ALMA for normal star-forming galaxies are the [O III] 88 μm and [C II] 158 μm fine structure lines, both of which are redshifted into the sub-mm atmospheric window in the reionization era. [C II] 158 μm is the dominant coolant of neutral gas in the ISM of local star-forming galaxies and its luminosity is observed to correlate closely with the star formation rate (SFR; De Looze et al. 2014). Early work exploring this relation at high redshifts revealed increased scatter compared to that seen in local samples. Whereas for luminous Lyman break galaxies selected at $z \simeq 5$–6 (e.g. Capak et al. 2015; Willott et al. 2015) as well as some Lyman-alpha emitters at $z \sim 6$ (Matthee et al. 2017; Carniani et al. 2018; Matthee et al. 2019) trends similar to those seen locally were found, other star-forming galaxies at $z > 6$ often showed weak or no [C II] 158 μm detections (e.g. Ota et al. 2014; Pentericci et al. 2016). This so-called '[C II]-deficit' has been the subject of much debate and was earlier discussed in the context of thermal saturation in ultra-luminous

★ E-mail: n.laporte@ucl.ac.uk

infrared galaxies (Muñoz & Oh 2016). While [C II] 158 μm is not affected by dust attenuation, it is sensitive to metallicity (Olsen et al. 2017), the ionization state of the gas (Vallini et al. 2017), and cosmic microwave background (CMB) attenuation. In addition, in a survey of three $z \simeq 7$ sources, Maiolino et al. (2015) discovered [C II] 158 μm emission with significant spatial offsets from the ultraviolet (UV) and Ly α emission, suggesting that the cores of young galaxies are disrupted by stellar feedback with line emission occurring only in external clumps of neutral gas. Although high-redshift data remain sparse and some non-detections are likely due to inadequate sensitivity, it remains of interest to pursue the topic to gain insight into the morphology and physical conditions in rapidly assembling young galaxies.

[O III] 88 μm emission also correlates with the star formation rate in local galaxies (De Looze et al. 2014) but, as a line with a higher ionization potential, it is generated within H II regions rather than in photodissociation regions. The motivation for targeting [O III] 88 μm at high redshift is two-fold. *Herschel* observations of dwarf galaxies suggested that it is a stronger line than [C II] 158 μm in low-metallicity systems (Madden et al. 2013). Additionally, the line is well placed observationally in the ALMA bands at the very highest redshifts for which targets are available from deep *Hubble* imaging. The line was prominently detected in two gravitationally lensed targets, A2744_YD4 at $z = 8.38$, for which a dust continuum detection was also secured (Laporte et al. 2017), and MACS1149_JD1 at $z = 9.11$ (Hashimoto et al. 2018). The two sources represent the highest redshift spectroscopically confirmed sources accessible to ALMA and in this paper we exploit the newly available band 5 receiver to present new observations targeting [C II] 158 μm in each source with the goal of further examining the relationship between [C II] 158 μm, [O III] 88 μm and various probes of star formation in early sources. Throughout the paper, we adopt a Λ-dominated, flat Universe with $\Omega_\Lambda = 0.7$, $\Omega_M = 0.3$, and $H_0 = 70\,\mathrm{km\,s^{-1}\,Mpc^{-1}}$.

2 OBSERVATIONS

Observations were carried out in band 5 during ALMA Cycles 5 and 6 under a regular proposal (2017.1.00697, PI: N. Laporte) and DDTs (2017.A.00026 and 2018.A.0004, PI: N. Laporte). The lower spectral window used to observe A2744_YD4 is centred on the frequency where [C II] 158 μm is expected at $z = 8.38$, and its width covers the redshift range $8.26 < z < 8.43$. The total exposure time on source was 3.8 h. A similar set-up was used for the MACS1149_JD1 observations, with a redshift range $8.96 \leq z \leq 9.16$ and a total exposure time of 6.2 h. Observations of A2744_YD4 were made with the C43-2 configuration yielding a beam size of 1.3 arcsec × 0.79 arcsec. For MACS1149_JD1, we used the configuration C43-4 to achieve a beam size of 0.75 arcsec × 0.63 arcsec. Data were reduced using the version 5.4.0 of the CASA pipeline (McMullin et al. 2007); a Briggs weighting was applied in the TCLEAN task in both cases. For consistency, we re-reduced ALMA band 7 data for A2744_YD4 following the same procedures (2015.1.00594, PI: N. Laporte)

We do not detect any band 5 continuum for either target. We measure 3σ upper limits using several beam-size apertures distributed at the centre of the field where our targets are located, and find $f_\nu^{158\,\mu\mathrm{m}} < 21\,\mu\mathrm{Jy\,beam^{-1}}$ for A2744_YD4 and $f_\nu^{158\,\mu\mathrm{m}} < 15\,\mu\mathrm{Jy\,beam^{-1}}$ for MACS1149_JD1 (not corrected for magnification). We also searched for line emission in a 1.5 arcsec radius circle around the UV rest-frame position of our targets (corresponding to a physical size of 13.2 and 14.1 kpc, respectively, for MACS1149_JD1 and A2744_YD4) allowing a velocity offset respective to the [O III] 88 μm redshift ranging from $-500\,\mathrm{km\,s^{-1}}$ to $500\,\mathrm{km\,s^{-1}}$ (e.g. Hashimoto et al. 2019). We rebinned the data assuming a full width at half-maximum (FWHM) of $100\,\mathrm{km\,s^{-1}}$ for [C II] 158 μm (as previously found for example in Carniani et al. 2017, Smit et al. 2018, and Bradač et al. 2017). No emission is detected in either target (Figs 1 and 2) with a 3σ upper limit on the [C II] 158 μm luminosity of $L_{\mathrm{C\,II}}^{\mathrm{JD1}} < 3.98 \times 10^6 \times (10/\mu)\,\mathrm{L_\odot}$ and $L_{\mathrm{C\,II}}^{\mathrm{YD4}} < 2.0 \times 10^7 \times (2/\mu)\,\mathrm{L_\odot}$, assuming an FWHM $= 100\,\mathrm{km\,s^{-1}}$, with the rms measured in several beam-size apertures (with $\theta_{\mathrm{min}} = 0.63$ arcsec and $\theta_{\mathrm{maj}} = 0.75$ arcsec for JD1 and $\theta_{\mathrm{min}} = 0.73$ arcsec and $\theta_{\mathrm{maj}} = 1.21$ arcsec) distributed in a 1.5 arcsec radius circle around the UV rest-frame position and taking into account the best magnification for the two targets ($\mu = 2$ and $\mu = 10$, respectively, for YD4 and JD1; see Laporte et al. 2017 and Hashimoto et al. 2018 for details). We also applied the same method to more finely binned data (FWHM $= 50\,\mathrm{km\,s^{-1}}$) taking into account the FWHM of the [O III] 88 μm line found in A2744_YD4, but no emission line was found on either data set.

We summarize the salient properties of A2744_YD4 and MACS1149_JD1 in Table 1. A similar non-detection of [C II] 158 μm was reported by Inoue et al. (2016) for a Ly α emitter at $z = 7.2$ with [O III] 88 μm emission and, in the following analysis, we include those measurements.

3 ANALYSIS

In Fig. 3 we compare the location of the two objects discussed in this paper, plus that of Inoue et al. (2016), in the [C II]–SFR relation traced at lower redshift. The apparent trend towards a [C II] deficit in the reionization era is striking. Likewise, Fig. 4 shows the [O III]/[C II] line ratio in the context of lower redshift metal-poor dwarf galaxies (Madden et al. 2013) and recent numerical simulations of high-redshift galaxies targeting both emission lines (Katz et al. 2019). The gas-phase metallicity in these simulations is 0.1 solar, comparable to that observed in the local dwarfs. Reducing the metallicity by a factor of 10 would be required to explain the absence of [C II] 158 μm although at that point [O III] 88 μm emission would be similarly reduced. Although it is possible that the [C II] 158 μm and [O III] 88 μm emission regions are physically distinct in some of our sources, these comparisons suggest that a low metallicity may be insufficient to explain the deficit. Additionally, the strongest likely attenuation of [C II] 158 μm by cosmic microwave background radiation (Lagache, Cousin & Chatzikos 2018) seems unable to explain the size of the discrepancy (see dashed lines in Fig. 4).

Energetic feedback from intermittent star formation may be capable of expelling neutral gas and thereby suppressing [C II] 158 μm emission. Although the presence of a significant dust mass in A2744_YD4 might then be considered surprising, the possibility of a spatial offset between [O III] 88 μm emission and the dust continuum (Fig. 2) may imply regions with different physical conditions or represent the result of some feedback process. One way to understand if a deficit of neutral gas is expected at high redshift is to determine the range of [C II] 158 μm emission expected in simulations. Examining a recent semi-analytical model of galaxy evolution (Lagache et al. 2018) in over 10^3 simulated objects at $z \simeq 8$ (Fig. 5) and focusing now only on the two highest redshift sources, A2744_YD4 and MACS1149_JD1, we find 75 simulated objects that have extreme properties similar to A2744_YD4 (i.e. SFR from 1 to $35\,\mathrm{M_\odot\,yr^{-1}}$; $L_{[\mathrm{C\,II}]} < 2.0 \times 10^7\,\mathrm{L_\odot}$; $\log(M_\star[\mathrm{M_\odot}])$ from 8.8 to 9.7) with mean properties $\langle M_\star \rangle = 1.3 \times 10^9\,\mathrm{M_\odot}$,

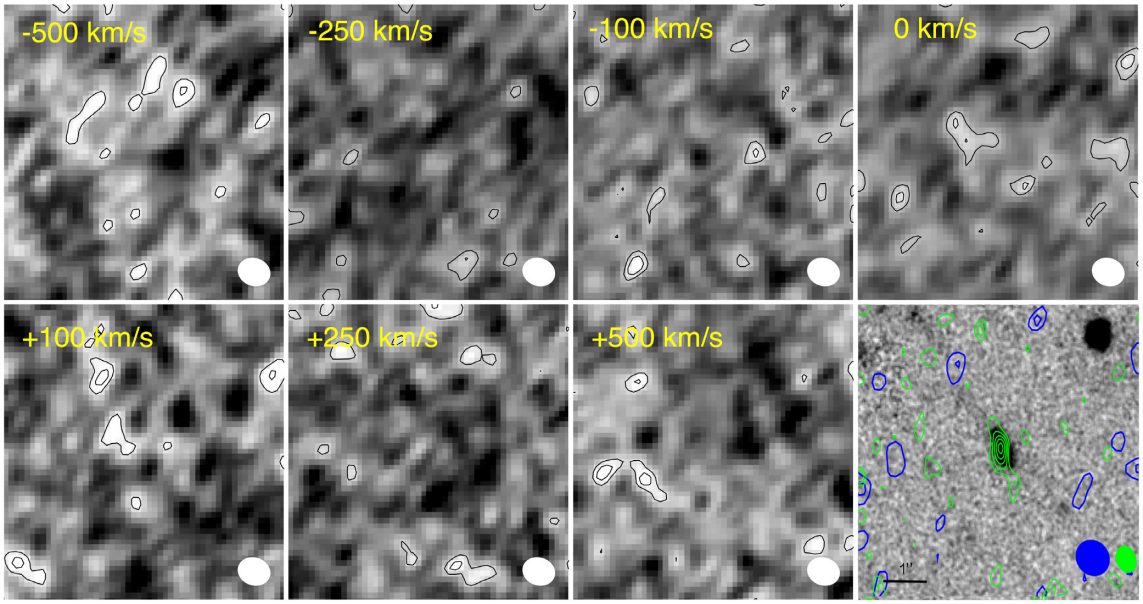

Figure 1. Search for [C II] 158 μm emission line near MACS1149_JD1. Each stamp shows the flux contours (drawn from 2σ) at different velocity offsets (from $-500\,\mathrm{km\,s^{-1}}$ to $+500\,\mathrm{km\,s^{-1}}$) with respect to the [O III] 88 μm redshift. The *HST* F160W image is shown at the bottom right of the figure with [O III] 88 μm (green) and [C II] 158 μm (blue) contours. The shape of the ALMA beam is placed at the bottom right of each ALMA stamp. No [C II] 158 μm emission is evident.

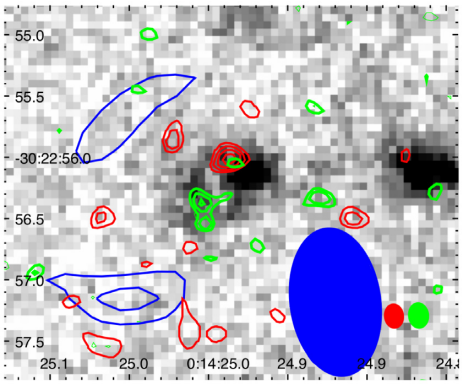

Figure 2. An ALMA view of A2744_YD4 showing the respective positions of the dust detection in ALMA band 7 (red), the [O III] 88 μm emission line (green) and the UV rest-frame continuum (*HST*/F160W image). The shape of each ALMA beam is shown at the bottom right. Contours are plotted from 2σ. No [C II] 158 μm emission (blue contours) is detected at more than 3σ near the rest-frame UV position of this galaxy.

Table 1. Properties of the two $z > 8$ galaxies reported in this paper. All values are corrected for magnification assuming $\mu = 2$ for A2744_YD4 and $\mu = 10$ for MACS1149_JD1.

	A2744_YD4	MACS1149_JD1
$z_{\mathrm{O\,III}}$	8.382^{a}	9.1096^{b}
$L_{\mathrm{O\,III}}$ ($\times 10^7\,\mathrm{L_\odot}$)	7.0 ± 1.7^{a}	7.4 ± 1.6^{b}
L_{FIR} ($\times 10^{10}\,\mathrm{L_\odot}$)	12.6 ± 5.5^{a}	$<0.77^{b}$
$L_{\mathrm{C\,II}}$ ($\times 10^7\,\mathrm{L_\odot}$)	<2.0 (3σ)	<0.4 (3σ)
$S_\nu^{158\,\mu\mathrm{m}}$ ($\mu\mathrm{Jy\,beam^{-1}}$)	<10.5 (3σ)	<1.5 (3σ)
$S_\nu^{88\,\mu\mathrm{m}}$ ($\mu\mathrm{Jy\,beam^{-1}}$)	99 ± 23 [a]	$<5.3^{b}$ (3σ)
SFR ($\mathrm{M_\odot\,yr^{-1}}$)	$20.4^{+17.6\,a}_{-9.5}$	$4.2^{+0.8\,b}_{-1.1}$
$M_\star$ ($10^9\,\mathrm{M_\odot}$)	$2.0^{+1.5\,a}_{-0.7}$	$1.1^{+0.5\,b}_{-0.2}$

[a] Laporte et al. (2017)
[b] Hashimoto et al. (2018)

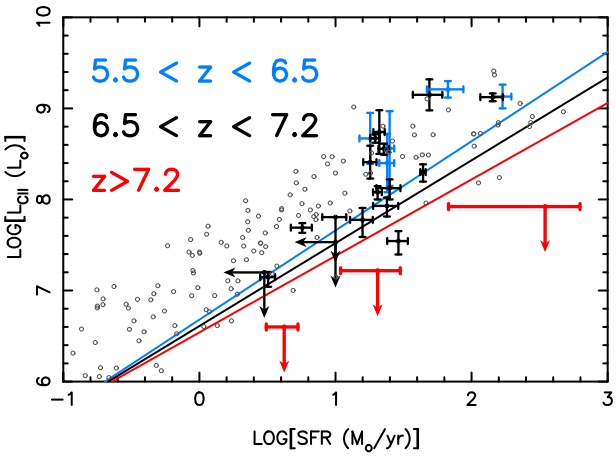

Figure 3. Relation between $L_{\mathrm{C\,II}}$ and the SFR for the two galaxies studied in this letter plus that of Inoue et al. (2016) (red) and previous $5.5 < z < 7.5$ galaxies studies from Capak et al. (2015), Carniani et al. (2017), Carniani et al. (2018), Smit et al. (2018), Pentericci et al. (2016), Hashimoto et al. (2019), Kanekar et al. (2013), Ota et al. (2014), Bradač et al. (2017), and Matthee et al. (2017) grouped according to redshift. Open circles show the location of local metal-poor dwarf galaxies (Madden et al. 2013). We also plot the relation predicted by Lagache et al. (2018) at $z \sim 6$ (blue), 7 (black), and 8 (red).

$\langle L_{[\mathrm{C\,II}]} \rangle = 9.4 \times 10^6$, and gas-phase metallicity $\langle Z_{\mathrm{g}} \rangle = 0.20$. Furthermore, only 8 simulated sources have [C II] 158 μm properties similar to MACS1149_JD1 (i.e. SFR from 0.9 to $6.6\,\mathrm{M_\odot\,yr^{-1}}$; $L_{[\mathrm{C\,II}]} < 0.4 \times 10^7\,\mathrm{L_\odot}$; $\log(M_\star[\mathrm{M_\odot}])$ from 8.7 to 9.4) with mean properties $\langle M_\star \rangle = 7.7 \times 10^8\,\mathrm{M_\odot}$, $\langle L_{[\mathrm{C\,II}]} \rangle = 2.7 \times 10^6\,\mathrm{L_\odot}$, and $\langle Z_{\mathrm{g}} \rangle = 0.25$. Since our observational upper limits are 3σ, this demonstrates the difficulty of reproducing our first glimpse at the weak [C II] 158 μm emission in $z > 8$ sources.

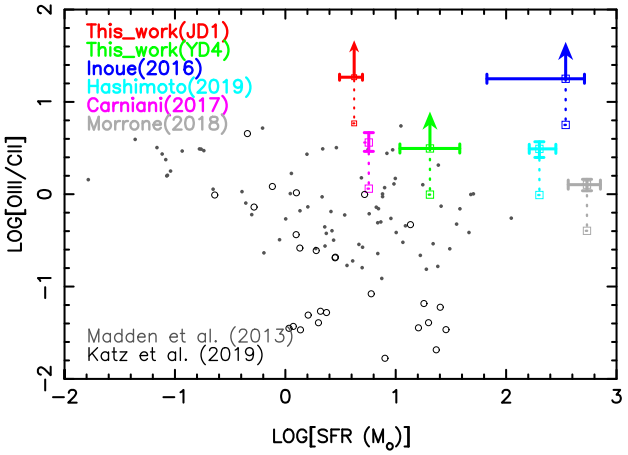

Figure 4. The [O III]/[C II] emission line ratio for high-redshift galaxies. Our work on MACS1149_JD1 and A2744_YD4 together with the $z = 7.2$ LAE (Inoue et al. 2016) indicates ratios well above those seen in local metal-poor dwarfs (Madden et al. 2013, grey circles) as well as numerical simulations capable of predicting both lines (Katz et al. 2019, black open symbols). The maximum effect of CMB attenuation is indicated by dashed lines below the current limits (see text for details).

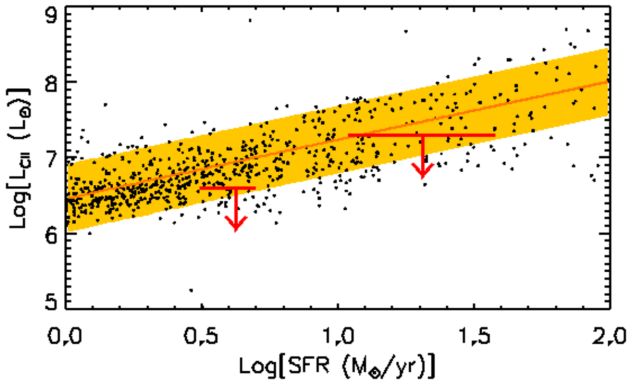

Figure 5. As Fig. 3 with the location of the two $z \geq 8$ galaxies discussed in this paper represented by red arrows. Black dots show the distribution of all the simulated galaxies from Lagache et al. (2018), extrapolated from their highest redshift $z = 7.6$ to redshift $z = 9$ by estimating a mean CMB attenuation factor on the [C II] 158 μm luminosity from $z = 7.6$ to $z = 9$. The red line displays the mean relation between the SFR and $L_{\rm C\,II}$ and the yellow region shows the mean dispersion (0.45 dex according to fig. 8 of Lagache et al. 2018) of the simulated galaxies. Clearly both galaxies are extreme outliers in the relation.

A further explanation may be a trend towards higher ionization parameters at early times (Katz 2016), for which there is some evidence in rest-frame UV spectroscopy of similar $z > 7$ sources (Mainali et al. 2018). Such a trend may arise from a moderate non-thermal component or an increasing contribution from metal-poor massive stars. The original motivation for this study was to assemble multiline data using ALMA for sources in the reionization era largely to test such hypotheses. Our discovery of a surprising [C II] 158 μm deficit argues for continuing this effort including further diagnostic lines sensitive to the nature of the radiation field, the gas-phase metallicity, and the presence of neutral gas.

Finally, utilizing the non-detection of the continuum of A2744_YD4 in ALMA band 5 we have the opportunity to reanalyse the SED of this object. We include data from a previous ALMA band 6 programme covering the position of this target (2015.1.00463.S, PI : M. Ouchi). In this data set, A2744_YD4 is also not detected and we measured in a beam-size aperture a 2σ upper limit flux of 30 μJy beam^{-1} (not corrected for magnification). Using *MAGPHYS* (da Cunha, Charlot & Elbaz 2008), we can give a first constraint on the dust temperature in this object, $T_{\rm dust} > 55$ K. This value contrasts with the value generally used to determine the dust properties at high z ($T \sim 30$ K), but is consistent with recent simulations (e.g. Behrens et al. 2018) which predict a higher dust temperature at high redshifts. Using the 3σ upper limits for both band 5 and 6 observations decreases the minimum dust temperature to $T > 43$ K.

4 SUMMARY

The recent commissioning of the ALMA band 5 receiver has opened a new window to study the ISM of the two most distant gravitationally lensed galaxies detected with ALMA band 7, namely A2744_YD4 ($z = 8.38$) and MACS1149_JD1 ($z = 9.11$). We have used this capability to search for the far-infrared (FIR) emission line [C II] 158 μm, the primary coolant of the ISM at low redshift, which should give valuable insight into the metallicity and neutral gas content for systems of known SFR. However, despite adequately sensitive data considering the [C II]–SFR relation observed at lower redshifts (e.g. $z < 6$), neither of these targets is detected in the dust continuum or line emission. Noting the magnification for these two targets ($\mu \sim 2$ and 10 for A2744_YD4 and MACS1149_JD1, respectively), these non-detections imply [C II]158 μm luminosities well below what is observed for $z \sim 0$ metal-poor dwarfs, reviving the discussion of a '[C II] deficit' previously considered at lower redshift. Likewise when studying the [O III] 88 μm/[C II] 158 μm line ratio, we find anomalously high values. We examine this line ratio with a recent hydrodynamical simulation of the ISM in early galaxies (Katz et al. 2019) and suggest that a low gas-phase metallicity may not be the sole explanation for this [C II] deficit. Other hypotheses include a high ionization parameter consistent with trends seen in UV spectroscopy of similar $z > 7$ sources or the suppression of neutral gas and hence [C II] 158 μm emission via energetic feedback from intermittent star formation. Using a semi-analytical model of galaxy evolution (Lagache et al. 2018), we demonstrate that such faint [C II] 158 μm luminosities are rarely expected at $z \geq 8$. Further multiline data on $z > 8$ sources will be helpful in resolving this puzzle. Our study emphasizes the importance of gathering multiline ALMA data for sources in the reionization era to robustly study the physical conditions in their interstellar media.

ACKNOWLEDGEMENTS

We thank Morgane Cousin for providing CMB attenuation estimates at $z \sim 9$. NL and RSE acknowledge funding from the European Research Council (ERC) under the European Union Horizon 2020 research and innovation programme (grant agreement No 669253). FEB acknowledges support from CONICYT-Chile (Basal AFB-170002, Programa de Cooperación Científica ECOS-CONICYT C16U02, FONDO ALMA 31160033) and the Ministry of Economy, Development, and Tourism's Millennium Science Initiative through grant IC120009, awarded to The Millennium Institute of Astrophysics, MAS. AKI and TH acknowledge funding from NAOJ ALMA Scientific Research Grant number 2016-01 A and JSPS KAKENHI Grant Number 17H01114. This paper makes use of the following ALMA data: ADS/JAO.ALMA#2015.A.00463, ADS/JAO.ALMA#2017.1.00697, ADS/JAO.ALMA#2017.A.00

026, and ADS/JAO.ALMA#2018.A.0004. ALMA is a partnership of ESO (representing its member states), NSF (USA), and NINS (Japan), together with NRC (Canada), MOST and ASIAA (Taiwan), and KASI (Republic of Korea), in cooperation with the Republic of Chile. The Joint ALMA Observatory is operated by ESO, AUI/NRAO, and NAOJ.

REFERENCES

Behrens C., Pallottini A., Ferrara A., Gallerani S., Vallini L., 2018, MNRAS, 477, 552
Bradač M. et al., 2017, ApJ, 836, L2
Capak P. L. et al., 2015, Nature, 522, 455
Carniani S. et al., 2017, A&A, 605, A42
Carniani S. et al., 2018, MNRAS, 478, 1170
da Cunha E., Charlot S., Elbaz D., 2008, MNRAS, 388, 1595
De Looze I. et al., 2014, A&A, 568, A62
Hashimoto T. et al., 2018, Nature, 557, 392
Hashimoto T. et al., 2019, preprint (arXiv:1806.00486)
Inoue A. K. et al., 2016, Science, 352, 1559
Kanekar N., Wagg J., Chary R. R., Carilli C. L., 2013, ApJ, 771, L20
Katz H., 2016, J. Br. Astron. Assoc., 126, 323
Katz H., Laporte N., Ellis R. S., Devriendt J., Slyz A., 2019, MNRAS, 484, 4054
Lagache G., Cousin M., Chatzikos M., 2018, A&A, 609, A130
Laporte N. et al., 2017, ApJ, 837, L21
Madden S. C. et al., 2013, PASP, 125, 600
Mainali R. et al., 2018, MNRAS, 479, 1180
Maiolino R. et al., 2015, MNRAS, 452, 54
Matthee J. et al., 2017, ApJ, 851, 145
Matthee J. et al., 2019, preprint (arXiv:1903.08171)
McMullin J. P., Waters B., Schiebel D., Young W., Golap K., 2007, in Shaw R. A., Hill F., Bell D. J., eds, ASP Conf. Ser. Vol. 376, Astronomical Data Analysis Software and Systems XVI. Astron. Soc. Pac., San Francisco, p. 127
Muñoz J. A., Oh S. P., 2016, MNRAS, 463, 2085
Olsen K., Greve T. R., Narayanan D., Thompson R., Davé R., Niebla Rios L., Stawinski S., 2017, ApJ, 846, 105
Ota K. et al., 2014, ApJ, 792, 34
Pavesi R., Riechers D. A., Faisst A. L., Stacey G. J., Capak P. L., 2018, preprint (arXiv:1812.00006)
Pentericci L. et al., 2016, ApJ, 829, L11
Smit R. et al., 2018, Nature, 553, 178
Tamura Y. et al., 2019, ApJ, 874, 27
Vallini L., Ferrara A., Pallottini A., Gallerani S., 2017, MNRAS, 467, 1300
Willott C. J., Carilli C. L., Wagg J., Wang R., 2015, ApJ, 807, 180

This paper has been typeset from a TEX/LATEX file prepared by the author.